Engineering Analysis with Boundary Elements 37 (2013) 527–541

Contents lists available at SciVerse ScienceDirect

Engineering Analysis with Boundary Elements

journal homepage: www.elsevier.com/locate/enganabound

Seepage analysis in multi-domain general anisotropic media by three-dimensional boundary elements

K. Rafiezadeh [a,*], B. Ataie-Ashtiani [a,b]

[a] Department of Civil Engineering, Sharif University of Technology, P.O. Box 11155-9313, Tehran, Iran
[b] National Centre for Groundwater Research & Training, Flinders University, GPO Box 2100, Adelaide, SA 5001, Australia

ARTICLE INFO

Article history:
Received 4 October 2012
Accepted 19 December 2012

Keywords:
Seepage
Boundary element method
Anisotropic
Multi-domain
Multi-region
Zoned
Dam
River
Well
Aquifer

ABSTRACT

A three-dimensional boundary element solution for the seepage analysis in multi-domain general anisotropic media has been developed based on the transformation approach. Using analytical eigenvalues and eigenvectors of the hydraulic conductivity tensor, a closed-form coordinate transformation matrix has been provided to transform the quadratic form of governing equation of seepage for the general anisotropic media to the Laplace equation. This transformation allows the analysis to be carried out using any standard BEM codes for the potential theory on the transformed space by adding small pre- and post-processing routines. With this transformation, any physical quantity like the total head remains unchanged at corresponding nodes on the physical and transformed space, and the normal gradient across the domain boundaries should also be transformed. In multi-domain problems, compatibility equations (equality of the potential on corresponding nodes on the interface) and equilibrium equations (conservation of the flux across the interface boundaries of adjacent domains) on the corresponding nodes of interface between two neighbor domains are needed for boundary element method. In the transformed space, the compatibility equation remains unchanged. However, due to the distortion of boundaries in the mapped space and therefore misalignment of the unit outward normal vectors along the inter-domain boundaries, the equilibrium of the normal fluxes have to be transformed accordingly. Based on the proposed transformation, the normal to boundary flux boundary conditions in the mapped space and the transformed equilibrium equation for interface of adjacent zones have been given in this paper. Examples have been solved with the proposed scheme and the results were verified with the finite element method. Excellent agreement of the results shows the veracity of the proposed transformation and the formulas given for transformation of equilibrium equation for multi-domain general anisotropic media.

1. Introduction

The boundary element method (BEM) was developed in the 1960s as an efficient numerical technic [1]. The method then has been used vastly for solving different problems in various fields. The method is of the great interest because of the numerical form of equations are written only on the domain boundaries. This allows for discretizing the just boundaries of the domain and there is no need for the discretization of the domain area. As modeling and discretization of the problem is one of the most costly parts of analyses [2], without the need of dealing with the interior mesh, the BEM is more cost effective in mesh preparation [1]. This is specially the case when working on three-dimensional problems when only surface boundaries are going to be discretized. In comparison with other numerical methods which mandates the discretization of the whole media such as finite element method (FEM), finite differences method (FDM) or control-volume method (CVM), the fewer numbers of nodes and elements in BEM not only reduces the costs of modeling and discretization, but also decreases the size of the problem which usually results in less computational efforts and memory storage for solution.

Boundary element method has been successfully used to solve Laplace equation in two- and three-dimensions [3]. As there are no body–forces in Laplace equation, when solving it with boundary element method, no domain integration is needed and all advantages of BEM are preserved. Governing equation of seepage in isotropic media is the Laplace equation: $\nabla^2\varphi = 0$ in which φ is the potential head [4]. BEM solution of seepage problems in isotropic two-dimensional problems are very well established in the literature, for example see [5,6]. In orthotropic materials that is a special case of anisotropy, the hydraulic conductivities are different in x, y and z directions but the principal axes of the hydraulic conductivities are parallel to the Cartesian system

* Corresponding author. Tel.: +98 9121977450.
E-mail address: rafiezadeh@gmail.com (K. Rafiezadeh).

0955-7997/$ - see front matter © 2013 Elsevier Ltd. All rights reserved.
http://dx.doi.org/10.1016/j.enganabound.2012.12.006

Nomenclature

x, y, z	coordinates in original domain
x_*, y_*, z_*	coordinates in rotated domain
x_{**}, y_{**}, z_{**}	coordinates in transformed domain
φ	potential head
p	seeping fluid pressure
ρ	seeping fluid density
$\mathbf{n}$	outward normal to boundary unit vector
$\mathbf{s}, \mathbf{t}$	two tangential to boundary unit vectors
$\partial\varphi/\partial n$	normal to boundary gradient of potential head
$\mathbf{q}$	flux vector
$\mathbf{K}$	hydraulic conductivity tensor
K_{xx}, K_{yy}, K_{zz}	diagonal elements of the hydraulic conductivity tensor
K_{xy}, K_{xz}, K_{yz}	cross-diagonal elements of the hydraulic conductivity tensor
$k_{x_*}, k_{y_*}, k_{z_*}$	hydraulic conductivity in principal axes directions
V_1, V_2, V_3	three eigenvectors of hydraulic conductivity tenor
∇	Nabla operator: $(\partial/\partial x,\ \partial/\partial y,\ \partial/\partial z)$
∇_2	horizontal gradient operator: $(\partial/\partial x,\ \partial/\partial y)$
∇^2	Laplacian operator: $\partial^2/\partial x^2+\partial^2/\partial y^2+\partial^2/\partial z^2$
G	Green's function
det[]	determinant operator of a matrix
I_1, I_2, I_3	invariants of hydraulic conductivity tensor
$\lambda_1, \lambda_2, \lambda_3$	three eigenvalues of hydraulic conductivity tensor
$\mathbf{R}$	rotating transformation matrix
$\mathbf{S}$	stretching transformation matrix
$\mathbf{T}$	direct transformation matrix

of coordinates. Governing equation in orthotropic media is $k_x\partial^2\varphi/\partial x^2+k_y\partial^2\varphi/\partial y^2+k_z\partial^2\varphi/\partial z^2=0$ [7], where k_x, k_y and k_z are the orthotropic hydraulic conductivities in x, y and z directions, respectively. Solution of this equation by boundary element method has been provided by two distinct approaches [8]. The first approach, that we here call it the fundamental solution approach, uses the fundamental solution of the governing equation. By the use of fundamental solution and the Green's theorem, the boundary integral equation can be derived. This boundary integral equation then can be discretized on the boundary for solving the problem by the boundary element method. Using this approach, Brebbia and Chang [7] derived $1/\{4\pi[k_xk_yk_z(x^2/k_x+y^2/k_z+z^2/k_z)]^{1/2}\}$ as the fundamental solution of the governing equation and then solved it directly by BEM. Weakly singular integral equations for Darcy's flow in anisotropic media are given in [9]. Rungamornrat [10] also used the fundamental solution approach and the governing equations were established based on a pair of weakly singular weak-form integral equations for fluid pressure and fluid flux. More complicated set of fundamental solutions for the problem were then used. The second approach, that we here call it the transformation approach, uses a mathematical transformation to transform the governing equation to Laplace equation. After transformation, the problem is solved by classical boundary element method for Laplace equation in the transformed space. Then by an inverse transformation, the calculated results will be transformed back to the original space. Transformation approach has also been used in [11–13] for seepage analysis with boundary elements in two-dimensional orthotropic materials. The transformation approach has been used successfully for seepage applications by Laef et.al. [14] for three-dimensional aquifers. Although the three-dimensional aquifers were dealt with in [14], the effective dimension of an aquifer system was reduced to two by use of the Dupuit assumptions. Laef et.al. [14] discussed that in many practical cases sufficiently accurate results could be obtained with less than a full three-dimensional analysis. Based on the fact that the horizontal dimensions of the aquifer are often much larger than the vertical dimensions, they assumed a 'nearly horizontal' flow as a good approximation. After assuming a nearly horizontal flow, their problem was reduced to two dimensions in the horizontal plane. They used the two-dimensional coordinate transformation to deal with anisotropy. Although the nearly horizontal assumption is a good approximation for some problems like large aquifers, in many other civil engineering structures like dams, sheet-piles, etc. it is not the case because the horizontal dimensions are not much larger than the vertical dimensions. Thus many problems can only be solved by a full three-dimensional analysis. A full three-dimensional seepage analysis of orthotropic materials by BEM has been given by Rafiezadeh and Ataie-Ashtiani [15] using the transformation approach. In their work they used the three-dimensional coordinate transformation for orthotropic materials to transform the governing equation to the Laplace equation.

For the well-posed seepage boundary value problems, the boundary conditions are of Dirichlet type (potential is prescribed) or Neumann type (normal to boundary potential gradient prescribed ($\partial\varphi/\partial n$)). In the fundamental solution approach however the required boundary condition should be one of the two cases: potential should be prescribed or $k_x\partial\varphi/\partial x+k_y\partial\varphi/\partial y+k_z\partial\varphi/\partial z$ should be prescribed [7]. In the second boundary condition type, most of the times the pre-calculation of the boundary condition should be done.

In the transformation approach, Dirichlet boundary condition remains unchanged while the Neumann boundary condition should also be transformed. The transformations of these Neumann boundary conditions are straight-forward and can easily be computed. The transformations are given for two-dimensions by Laef et.al.[14] and Liggett and Liu [5] for general anisotropic media. In three-dimensions, such transformations for orthotropic media are given by Rafiezadeh and Ataie-Ashtiani [15]. In multi-domain problems, corresponding nodes on the interface between neighboring domains should satisfy the compatibility and equilibrium equations. Compatibility equations oblige the equality of the potential on adjacent nodes and equilibrium conditions conserve the flowing normal flux between the two neighboring domains. For any seepage analysis in multi-domain media by BEM, the compatibility and equilibrium equations should be undertaken in the model. When the domains are anisotropic and the transformation approach is used, these equations should also be transformed. The compatibility equation remains unchanged after transformation however, the distortion of boundaries leads to misalignment of the unit outward normal vectors along the interfaces of neighboring domains, the equilibrium of normal fluid fluxes needs to be transformed accordingly. $(k_{xx}^{(1)}k_{yy}^{(1)})^{1/2}(\partial\varphi/\partial n)^{(1)}=(k_{xx}^{(2)}k_{yy}^{(2)})^{1/2}(\partial\varphi/\partial n)^{(2)}$ has been used as the equilibrium equation in [11–13] which is an approximation based on the concept of equivalent hydraulic conductivity in two-dimensional orthotropic domains. Laef et.al. [14] derived the exact transformation of equilibrium equation in two dimensions. Rafiezadeh and Ataie-Ashtiani [15] derived the exact equilibrium condition for three-dimensional orthotropic media.

More general anisotropic media often occur when dealing with applied seepage problems in engineering. Large hydraulic structures like dams are usually built on the rivers flowing in young

geological areas. The foundations of dams are usually made from layers of folded deposited sediments. Sedimentary deposits are often anisotropic with flow occurring more readily along the plane of deposition than across it [16]. When such layers are folded, the principal axes of hydraulic conductivity do not remain horizontal or vertical and so the media cannot be assumed as orthotropic media and cases of general anisotropy happen. Underground water supply projects are also the similar case while pumping out the water are often happened through wells that are drilled into folded aquifers. In such media that are not orthotropic, the conductivity tensor is not diagonal and the cross-diagonal elements do not vanish. In this case of general anisotropy the governing equation of seepage will be $k_{xx}\partial^2\varphi/\partial x^2+k_{yy}\partial^2\varphi/\partial y^2+k_{zz}\partial^2\varphi/\partial z^2+2k_{xy}\partial^2\varphi/\partial x\partial y+2k_{yz}\partial^2\varphi/\partial y\partial z+2k_{xz}\partial^2\varphi/\partial x\partial z=0$.

Although this equation of seepage has been numerously solved by the finite element method, reports of solution by boundary element method are very sparse in the literature. A fundamental solution approach has been used to solve the anisotropic potential problems with indirect BEM by Zhang et.al. [17]. A comparison of boundary element method formulations for steady state anisotropic heat conduction in two dimensions based on the fundamental solution has been given by Mera et.al. [8]. Fundamental solution for the general anisotropic Laplacian operator has been given by [18,19]. Solution of this equation by the fundamental solution approach has recently been presented by [19] for applications in heat conduction problems. The presented fundamental solution for the equation is $1/\{4\pi[x^2(k_{yy}\ k_{zz}-k_{yz}^2)+y^2(k_{xx}\ k_{zz}-k_{xz}^2)+z^2(k_{xx}k_{yy}-k_{xy}^2)+2xy(k_{xy}k_{zz}-k_{xz}\ k_{yz})+2yz(k_{xx}k_{yz}-k_{xy}\ k_{xz})+2xz(k_{xy}k_{yz}-k_{xz}k_{yy})]^{1/2}\}$. Although they derived the fundamental solution for the three-dimensional general anisotropic Laplacian operator, their work was about two-dimensional anisotropic Poisson problems.

An engineer may decide to use (i) the principal directions as the coordinate axes (instead of the usual horizontal and vertical) of choice in describing the 3D geometry of the model, (ii) make use of the principal permeability in transforming the geometry into an equivalent isotropic medium (stretching transformation) and (iii) solve the problem, the results will match with the use of the proposed direct transformation. The transformations for this method of solution are detailed in [15]. However use of the direct transformation encapsulates the pre-processing and post-processing tasks of the engineer into the closed-form formulations of the direct transformation. Especially, when dealing with multi-domain problems that each domain has a different conductivity tensor, multiple coordinate axes should be defined (a coordinate system per each domain) and this makes the tasks heavier and following the direct transformation procedure can reduce the required efforts significantly.

Using the transformation approach in BEM context, combination of a rotation with a stretching of coordinates has been used by Liggett and Liu [5] to transform the two-dimensional general anisotropic governing equation to the Laplace equation. Transformation of the flux boundary conditions is also presented in their work for two dimensions. Shiah and Tan [20] used a different coordinate transformation to transform the governing equation to the Laplace equation in two dimensions. They derived this transformation from the method of characteristics. Hsieh and Ma [21] introduced a linear coordinate transformation method to solve the heat conduction on a thin layer of anisotropic medium subjected to arbitrary thermal loadings applied inside the domain or on the boundary surfaces. Ma and Chang [22] studied the two-dimensional steady-state thermal conduction problems in the anisotropic multi-layered media. They have used the linear coordinate transformation to simplify the governing equation without complicating the boundary and interface conditions. Shiah and Tan [23] extended their earlier two-dimensional work to three-dimensional anisotropic field problems. To calculate the normal to boundary gradient in the distorted model they provided a formula in terms of $\partial\varphi/\partial x$, $\partial\varphi/\partial y$ and $\partial\varphi/\partial z$ on the physical domain. After solving the distorted model, for inverse transformation and calculating the $\partial\varphi/\partial n$ on the physical domain, they provided another formula in terms of $\partial\varphi/\partial\hat{\xi}$, $\partial\varphi/\partial\hat{\eta}$ and $\partial\varphi/\partial\hat{n}$ on the distorted model. In the proposed formula, the potential gradient $\partial\varphi/\partial\hat{n}$ is directly obtained from the solution of the boundary integral equation for the distorted domain, while the other two potential gradients $\partial\varphi/\partial\hat{\xi}$ and $\partial\varphi/\partial\hat{\eta}$ can be computed using the standard numerical interpolation scheme involving the shape functions. Their work was for single-domain problems and they have not provided the transformation of the compatibility and equilibrium conditions. In their work, they only concentrated on single domain media and mentioned that additional conditions that invoke equilibrium and compatibility of the potential gradient and the potential, respectively, at the interface boundaries must be specified and because of the distortion of the domain in the mapped plane, they are relatively more complicated in form when compared to the isotropic case and so this issue was outside the scope of the their study and thus was not addressed in their paper [23]. Shiah et.al. [24] then provided the complete transformations for heat flux boundary conditions for the linear coordinate transformations provided in [20,23] for 2D and 3D cases respectively. They also derived the transformed compatibility and equilibrium conditions needed for the standard multi-domain BEM for heat conduction problems.

To the best of authors' knowledge, no BEM solution for the fully anisotropic seepage problems has been given in multi-domain three-dimensional media yet. The main objective of this study is to develop a BEM solution for seepage in three-dimensional multi-domain general anisotropic media. As mentioned before, despite the obvious importance of three-dimensional boundary element method implementations, most of the BEM developments in seepage analysis have been done in two dimensions. In this study we apply the transformation approach in three dimensions. We provide a direct transformation to map the general anisotropic governing equation of seepage to the familiar Laplace equation. By using analytical closed-form eigenvectors of the hydraulic conductivity tensor, the transformation matrix that rotates the system of coordinates to the principal axes of the hydraulic conductivities is derived analytically. This first step transforms the quadratic form of the governing equation to the canonic form. A further coordinate stretching transformation can be used to transform the canonic form to the Laplace equation [15]. By combining these two transformations into one transformation, a single-step closed-form transformation has been provided that can directly transform the quadratic governing equation to the Laplace equation. Using this transformation, the potential boundary conditions remain unchanged, but the flux boundary conditions should be transformed accordingly. Transformation of the flux boundary conditions is derived analytically. We show that when using the specific provided transformation, the transformed normal to boundary flux boundary condition in the distorted domain is a function of normal to boundary flux in the physical domain only and neither tangential fluxes nor $\partial\varphi/\partial x$, $\partial\varphi/\partial y$ or $\partial\varphi/\partial z$ are needed in physical or distorted models for transform (physical to distorted) and inverse-transform (distorted to physical) and this is an advantage of this transformation in comparison with the transformation proposed in [23]. For providing a complete BEM solution to the multi-domain problems, the new compatibility conditions (Equality of the potential on adjacent nodes on neighbor domains) and equilibrium conditions (conservation of the flowing flux) should also be transformed. Compatibility conditions remain unchanged in the transformed domain, but the equilibrium

condition will change. To extend our previous study in orthotropic media [15], the transformed equilibrium equation is provided in this paper for the general anisotropic case. To verify our formulations and the proposed BEM solution for the single- and multi-domain three-dimensional general anisotropic problems, three numerical examples will be presented. The formulation detailed in [15] is a special case of the formulations that are presented in this paper. If a media with a horizontal and vertical principal hydraulic coordinates exists or using the aligned principal hydraulic conductivities as the coordinate axes for geometry definition (i.e. the off-diagonal terms will be zero) the proposed formulations will reduce to the ones presented in [15]. The examples are solved with BEM with the transformations proposed and are verified with comparison to the FEM results. The examples were chosen to address the most important cases of general anisotropic problems in real seepage applications in civil engineering practice which are wells and dam-sites.

2. Governing equation

We can define the specific discharge **q** (or seepage velocity) as the volume flow rate per unit total area (pores plus particles) normal to the flow. Assuming that the averaged flow field can be considered as a continuum and applying the principle of mass conservation and assuming saturated flows and neglecting fluid and soil compressibility, we can derive the following equation [5]:

$$\nabla \mathbf{q} = 0 \tag{1}$$

Darcy's law says

$$\mathbf{q} = -\mathbf{K}\nabla\varphi \tag{2}$$

in which φ is the potential head which is defined by $\varphi = p/\rho g + z$ in which p is the fluid pressure, ρ is the density of fluid, g is the gravity and **K** is the permeability or hydraulic conductivity tensor defined as follows:

$$\mathbf{K} = \begin{bmatrix} k_{xx} & k_{xy} & k_{xz} \\ k_{xy} & k_{yy} & k_{yz} \\ k_{xz} & k_{yz} & k_{zz} \end{bmatrix} \tag{3}$$

The cross-permeability, i.e. the off-diagonal term in the hydraulic conductivity tensor are symmetric. A simple interpretation of the off-diagonal terms is that k_{xy}, for example, is the hydraulic conductivity value determining the specific discharge in the x-direction due to a hydraulic gradient directed along the y-coordinate axis [25]. To determine the hydraulic conductivity tensor in three dimensions by in-situ tests, one may use aquifer pumping test or packer test data based on the assumption that the groundwater is flowing through a geologic continuum [26,27]. Estimation of three-dimensional hydraulic conductivity tensor through a single well packer test and discrete fracture fluid flow modeling is also applicable for a fractured rock mass [28].

Combining Eqs. (1) and (2) we may have:

$$\nabla(\mathbf{K}\nabla\varphi) = 0 \tag{4}$$

Assuming homogeneity of hydraulic conductivity tensor, by expanding Eq. (4) and substituting **K** from Eq. (3), one can find the governing equation for seepage in general anisotropic media as following:

$$k_{xx}\frac{\partial^2\varphi}{\partial x^2} + k_{yy}\frac{\partial^2\varphi}{\partial y^2} + k_{zz}\frac{\partial^2\varphi}{\partial z^2} + 2k_{xy}\frac{\partial^2\varphi}{\partial x\partial y} + 2k_{yz}\frac{\partial^2\varphi}{\partial y\partial z} + 2k_{xz}\frac{\partial^2\varphi}{\partial x\partial z} = 0 \tag{5}$$

3. Domain transformation

We want to seek a coordinate transformation to transform the governing Eq. (5) to a standard Laplace equation. The governing equation has a quadratic form and can be transformed to canonic form by the following transformation [29]:

$$\begin{Bmatrix} x_* \\ y_* \\ z_* \end{Bmatrix} = \begin{bmatrix} \{V_1\}^T \\ \{V_2\}^T \\ \{V_3\}^T \end{bmatrix} \begin{Bmatrix} x \\ y \\ z \end{Bmatrix} \tag{6}$$

In which $\{V_1\}$, $\{V_2\}$ and $\{V_3\}$ are the eigenvectors of the hydraulic conductivity tensor. The above coordinate transformation will transform the governing equation to the following canonical form:

$$k_{x_*}\frac{\partial^2\varphi}{\partial x_*^2} + k_{y_*}\frac{\partial^2\varphi}{\partial y_*^2} + k_{z_*}\frac{\partial^2\varphi}{\partial z_*^2} = 0 \tag{7}$$

In which k_{x_*}, k_{y_*} and k_{z_*} are the principal hydraulic conductivities. This transformation is a rotating transform which rotates the coordinate system to a new one that the axes are parallel to the principal axes of the conductivity tensor.

To transform Eq. (7) to the Laplace equation a further coordinate transformation in the following form is applied:

$$x_{**} = x_*(k_{z_*}/k_{x_*})^{1/2} \tag{8}$$

$$y_{**} = y_*(k_{z_*}/k_{y_*})^{1/2} \tag{9}$$

$$z_{**} = z_* \tag{10}$$

This second transformation is a stretching transformation that stretches x_*, y_* and z_* coordinates to x_{**}, y_{**} and z_{**}coordinates. In the transformed coordinates, the governing equation will be:

$$\frac{\partial^2\varphi}{\partial x_{**}^2} + \frac{\partial^2\varphi}{\partial y_{**}^2} + \frac{\partial^2\varphi}{\partial z_{**}^2} = 0 \tag{11}$$

Rotating and stretching transformations of coordinate axes are shown schematically in Fig. 1. To obtain a transformation that directly transforms our governing equation to Laplace equation we firstly use the analytical eigenvectors and eigenvalues of the conductivity tensor [30].

The Cartesian hydraulic conductivity tensor **K** has three principal invariants, $\{I_1,I_2,I_3\}$, which are related to the eigenvalues, $\{\lambda\}$ and defined by the characteristic equation [31]

$$\det[\mathbf{K}-\lambda\mathbf{I}_{3\times3}] = (\lambda-\lambda_1)(\lambda-\lambda_2)(\lambda-\lambda_3) = \lambda^3 - I_1\lambda^2 + I_2\lambda - I_3 = 0 \tag{12}$$

where $\mathbf{I}_{3\times3}$ is the 3×3 identity matrix. From the equation above the three invariants are given by [31]

$$I_1 = k_{xx} + k_{yy} + k_{zz} \tag{13}$$

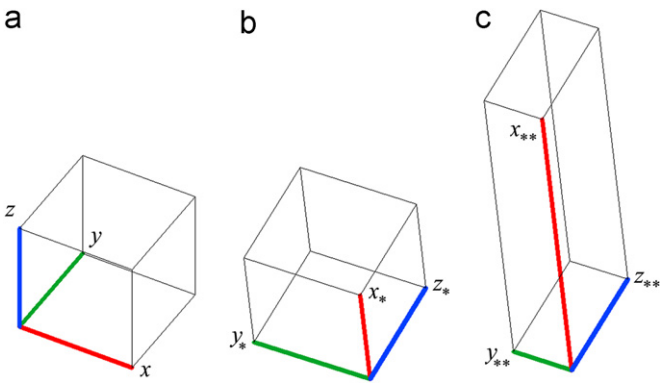

Fig. 1. (a) Original coordinates, (b) rotated coordinates, (c) rotated then stretched coordinates.

$$I_2 = k_{xx}k_{yy} + k_{yy}k_{zz} + k_{zz}k_{xx} - k_{xy}^2 - k_{yz}^2 - k_{xz}^2 \tag{14}$$

$$I_3 = k_{xx}k_{yy}k_{zz} + 2k_{xy}k_{yz}k_{xz} - (k_{xx}k_{yz}^2 + k_{yy}k_{xz}^2 + k_{zz}k_{xy}^2) \tag{15}$$

The analytical solution presented here is specific to the positive-definite and symmetric Cartesian tensors that are commonly encountered in many applications including seepage, diffusion and heat conduction.

We then define the following additional auxiliary variables [30]:

$$v = (I_1/3)^2 - I_2/3 \tag{16}$$

$$s = (I_1/3)^3 - I_1 I_2/6 + I_3/2 \tag{17}$$

$$\theta = \frac{1}{3}\cos^{-1}\left(\frac{s}{v^{3/2}}\right) \tag{18}$$

As these three variables are functions of I_1,I_2 and I_3 only, they are also rotationally invariant parameters. The three eigenvalues of the conductivity tensor which are the principal hydraulic conductivities of the media then can be calculated as following [30]:

$$k_{x_*} = \lambda_1 = \frac{I_1}{3} + 2\sqrt{v}\cos\theta \tag{19}$$

$$k_{y_*} = \lambda_2 = \frac{I_1}{3} - 2\sqrt{v}\cos\left(\theta + \frac{\pi}{3}\right) \tag{20}$$

$$k_{z_*} = \lambda_3 = I_1 - k_{x_*} - k_{y_*} \tag{21}$$

After the three eigenvalues have been computed, the three eigenvectors $\{V_1\}$, $\{V_2\}$ and $\{V_3\}$ can be calculated from the following equations [30]:

$$[K]\{V_1\} = k_{x_*}\{V_1\} \tag{22}$$

$$[K]\{V_2\} = k_{y_*}\{V_2\} \tag{23}$$

$$[K]\{V_3\} = k_{z_*}\{V_3\} \tag{24}$$

Solving the above equations for eigenvectors gives the analytical eigenvectors as the following:

$$\{V_1\} = \begin{Bmatrix} V_{1x} & V_{1y} & V_{1z} \end{Bmatrix}^{\mathrm{T}} \tag{25}$$

$$\{V_2\} = \begin{Bmatrix} V_{2x} & V_{2y} & V_{2z} \end{Bmatrix}^{\mathrm{T}} \tag{26}$$

$$\{V_3\} = \begin{Bmatrix} V_{3x} & V_{3y} & V_{3z} \end{Bmatrix}^{\mathrm{T}} \tag{27}$$

in which

$$V_{1x} = [k_{xy}k_{yz} - B_x k_{xz}][k_{yz}k_{xz} - C_x k_{xy}] \tag{28}$$

$$V_{1y} = [k_{yz}k_{xz} - C_x k_{xy}][k_{xz}k_{xy} - A_x k_{yz}] \tag{29}$$

$$V_{1z} = [k_{xz}k_{xy} - A_x k_{yz}][k_{xy}k_{yz} - B_x k_{xz}] \tag{30}$$

$$V_{2x} = [k_{xy}k_{yz} - B_y k_{xz}][k_{yz}k_{xz} - C_y k_{xy}] \tag{31}$$

$$V_{2y} = [k_{yz}k_{xz} - C_y k_{xy}][k_{xz}k_{xy} - A_y k_{yz}] \tag{32}$$

$$V_{2z} = [k_{xz}k_{xy} - A_y k_{yz}][k_{xy}k_{yz} - B_y k_{xz}] \tag{33}$$

$$V_{3x} = [k_{xy}k_{yz} - B_z k_{xz}][k_{yz}k_{xz} - C_z k_{xy}] \tag{34}$$

$$V_{3y} = [k_{yz}k_{xz} - C_z k_{xy}][k_{xz}k_{xy} - A_z k_{yz}] \tag{35}$$

$$V_{3z} = [k_{xz}k_{xy} - A_z k_{yz}][k_{xy}k_{yz} - B_z k_{xz}] \tag{36}$$

$$A_x = k_{xx} - k_{x_*} \tag{37}$$

$$A_y = k_{xx} - k_{y_*} \tag{38}$$

$$A_z = k_{xx} - k_{z_*} \tag{39}$$

$$B_x = k_{yy} - k_{x_*} \tag{40}$$

$$B_y = k_{yy} - k_{y_*} \tag{41}$$

$$B_z = k_{yy} - k_{z_*} \tag{42}$$

$$C_x = k_{zz} - k_{x_*} \tag{43}$$

$$C_y = k_{zz} - k_{y_*} \tag{44}$$

$$C_z = k_{zz} - k_{z_*} \tag{45}$$

Due to Eq. (6), the rotation transformation matrix **R** which rotates the coordinate axes parallel to the principal axes of the hydraulic conductivity tensor then will be equal to:

$$\mathbf{R} = \begin{bmatrix} V_{1x} & V_{1y} & V_{1z} \\ V_{2x} & V_{2y} & V_{2z} \\ V_{3x} & V_{3y} & V_{3z} \end{bmatrix} \tag{46}$$

And thus we will have

$$\begin{Bmatrix} x_* \\ y_* \\ z_* \end{Bmatrix} = \mathbf{R}\begin{Bmatrix} x \\ y \\ z \end{Bmatrix} \tag{47}$$

If we write the stretching transformation that is given in Eqs. (8)–(10) in the matrix form, we will have

$$\begin{Bmatrix} x_{**} \\ y_{**} \\ z_{**} \end{Bmatrix} = \mathbf{S}\begin{Bmatrix} x_* \\ y_* \\ z_* \end{Bmatrix} \tag{48}$$

in which **S**, the stretching transformation matrix is defined by

$$\mathbf{S} = \begin{bmatrix} (k_{z_*}/k_{x_*})^{\frac{1}{2}} & 0 & 0 \\ 0 & (k_{z_*}/k_{y_*})^{\frac{1}{2}} & 0 \\ 0 & 0 & 1 \end{bmatrix} \tag{49}$$

Transformation matrix **T** is then defined as the following:

$$\mathbf{T} = \mathbf{S} \times \mathbf{R} \tag{50}$$

Combining Eqs. (47), (48) and (50) one may have:

$$\begin{Bmatrix} x_{**} \\ y_{**} \\ z_{**} \end{Bmatrix} = \mathbf{T}\begin{Bmatrix} x \\ y \\ z \end{Bmatrix} \tag{51}$$

in which **T** can be calculated by substituting (46) and (49) in (50):

$$\mathbf{T} = \begin{bmatrix} (k_{z_*}/k_{x_*})^{\frac{1}{2}}V_{1x} & (k_{z_*}/k_{x_*})^{\frac{1}{2}}V_{1y} & (k_{z_*}/k_{x_*})^{\frac{1}{2}}V_{1z} \\ (k_{z_*}/k_{y_*})^{\frac{1}{2}}V_{2x} & (k_{z_*}/k_{y_*})^{\frac{1}{2}}V_{2y} & (k_{z_*}/k_{y_*})^{\frac{1}{2}}V_{2z} \\ V_{3x} & V_{3y} & V_{3z} \end{bmatrix} \tag{52}$$

Transformation (51) is a direct transformation that transforms the governing Eq. (5) to the Laplace Eq. (11).

4. Transformation of Neumann boundary condition

When the transformation in Eq. (51) is used, the domain will be transformed to a distorted one. To solve the problem on the transformed domain, we have to know the boundary conditions on the transformed domain boundary, thus we should also transform the boundary conditions accordingly. We usually have two types of boundary conditions, the Dirichlet boundary conditions and the Neumann boundary conditions. The Dirichlet boundary condition will remain unchanged when the coordinate transformation (51) is used because the physical quantity of potential head is independent form the geometry and remain

unchanged at corresponding points on the physical and transformed domains. But because of the distortion in the domain, the normal to boundary vectors will change and thus the potential gradient across the boundaries will change accordingly. Thus the Neumann boundary conditions should be transformed and the appropriate $\partial\varphi/\partial n_{**}$ should be calculated.

As mentioned in the previous section the transformation **T** is in fact the combination of two successive rotation **R** and stretching **S** transformations which are defined in Eqs. (47) and (48) respectively. When the domain is rotated, no distortion happens in the domain and potential normal gradients remain unchanged, i.e.

$$\partial\varphi/\partial n = \partial\varphi/\partial n_{*} \tag{53}$$

But when the coordinate stretching transformation acts, the domain will be distorted the normal to boundary unit vectors change and thus the potential normal gradients will change as well, i.e.

$$\partial\varphi/\partial n_{*} \neq \partial\varphi/\partial n_{**} \tag{54}$$

To calculate the transformed value of the Neumann boundary conditions in terms of values of the Neumann boundary conditions in the original domain, consider

$$\alpha = (k_{z_*}/k_{x_*})^{1/2} \tag{55}$$

$$\beta = (k_{z_*}/k_{y_*})^{1/2} \tag{56}$$

Using Eqs. (8)–(10) and the chain rule in differentiation we will have

$$\frac{\partial\varphi}{\partial x_*} = \alpha\frac{\partial\varphi}{\partial x_{**}} \tag{57}$$

$$\frac{\partial\varphi}{\partial y_*} = \beta\frac{\partial\varphi}{\partial y_{**}} \tag{58}$$

$$\frac{\partial\varphi}{\partial z_*} = \frac{\partial\varphi}{\partial z_{**}} \tag{59}$$

We also have

$$\begin{aligned}
\frac{\partial\varphi}{\partial x_{**}} &= \frac{\partial\varphi}{\partial n_{**}}n_{x_{**}} + \frac{\partial\varphi}{\partial s_{**}}s_{x_{**}} + \frac{\partial\varphi}{\partial t_{**}}t_{x_{**}}\\
\frac{\partial\varphi}{\partial y_{**}} &= \frac{\partial\varphi}{\partial n_{**}}n_{y_{**}} + \frac{\partial\varphi}{\partial s_{**}}s_{y_{**}} + \frac{\partial\varphi}{\partial t_{**}}t_{y_{**}}\\
\frac{\partial\varphi}{\partial z_{**}} &= \frac{\partial\varphi}{\partial n_{**}}n_{z_{**}} + \frac{\partial\varphi}{\partial s_{**}}s_{z_{**}} + \frac{\partial\varphi}{\partial t_{**}}t_{z_{**}}
\end{aligned} \tag{60}$$

where

$$\begin{aligned}
&n_{x_{**}} = \mathbf{n}_{**}.\mathbf{i}, \quad n_{y_{**}} = \mathbf{n}_{**}.\mathbf{j}, \quad n_{z_{**}} = \mathbf{n}_{**}.\mathbf{k}\\
&s_{x_{**}} = \mathbf{s}_{**}.\mathbf{i}, \quad s_{y_{**}} = \mathbf{s}_{**}.\mathbf{j}, \quad s_{z_{**}} = \mathbf{s}_{**}.\mathbf{k}\\
&t_{x_{**}} = \mathbf{t}_{**}.\mathbf{i}, \quad s_{y_{**}} = \mathbf{t}_{**}.\mathbf{j}, \quad s_{z_{**}} = \mathbf{t}_{**}.\mathbf{k}
\end{aligned} \tag{61}$$

and **n** is the unit normal to boundary vector and **s** and **t** are the two tangential unit vectors of the boundary. We also have

$$\frac{\partial\varphi}{\partial n_*} = \frac{\partial\varphi}{\partial x_*}n_{x_*} + \frac{\partial\varphi}{\partial y_*}n_{y_*} + \frac{\partial\varphi}{\partial z_*}n_{z_*} \tag{62}$$

Using Eqs. (57)–(59) in Eq. (62) we will have

$$\frac{\partial\varphi}{\partial n_*} = \alpha\frac{\partial\varphi}{\partial x_{**}}n_{x_*} + \beta\frac{\partial\varphi}{\partial y_{**}}n_{y_*} + \frac{\partial\varphi}{\partial z_{**}}n_{z_*} \tag{63}$$

Substituting $\partial\varphi/\partial x_{**}$, $\partial\varphi/\partial y_{**}$ and $\partial\varphi/\partial z_{**}$ from Eq. (60) into Eq. (63) and rearranging will give

$$\begin{aligned}
\frac{\partial\varphi}{\partial n_*} = &\frac{\partial\varphi}{\partial n_{**}}(\alpha n_{x_*}n_{x_{**}} + \beta n_{y_*}n_{y_{**}} + n_{z_*}n_{z_{**}})\\
&+ \frac{\partial\varphi}{\partial s_{**}}(\alpha n_{x_*}s_{x_{**}} + \beta n_{y_*}s_{y_{**}} + n_{z_*}s_{z_{**}})\\
&+ \frac{\partial\varphi}{\partial t_{**}}(\alpha n_{x_*}t_{x_{**}} + \beta n_{y_*}t_{y_{**}} + n_{z_*}t_{z_{**}})
\end{aligned} \tag{64}$$

From definition of stretching transformation we have

$$\begin{aligned}
&\frac{s_{x_*}}{s_{z_*}} = \alpha\frac{s_{x_{**}}}{s_{z_{**}}}, \quad \frac{t_{x_*}}{t_{z_*}} = \alpha\frac{t_{x_{**}}}{t_{z_{**}}}, \quad \frac{n_{z_*}}{n_{x_*}} = \alpha\frac{n_{z_{**}}}{n_{x_{**}}}\\
&\frac{s_{y_*}}{s_{z_*}} = \beta\frac{s_{y_{**}}}{s_{z_{**}}}, \quad \frac{t_{y_*}}{t_{z_*}} = \beta\frac{t_{y_{**}}}{t_{z_{**}}}, \quad \frac{n_{z_*}}{n_{y_*}} = \beta\frac{n_{z_{**}}}{n_{y_{**}}}
\end{aligned} \tag{65}$$

Using (65), we may have

$$\begin{aligned}
\alpha n_{x_*}s_{x_{**}} + \beta n_{y_*}s_{y_{**}} + n_{z_*}s_{z_{**}} &= s_{z_{**}}(\alpha n_{x_*}s_{x_{**}}/s_{z_{**}} + \beta n_{y_*}s_{y_{**}}/s_{z_{**}} + n_{z_*})\\
&= s_{z_{**}}(n_{x_*}s_{x_*}/s_{z_*} + n_{y_*}s_{y_*}/s_{z_*} + n_{z_*}) = \frac{s_{z_{**}}}{s_{z_*}}\,\mathbf{n}_*.\mathbf{s}_*
\end{aligned} \tag{66}$$

From the normality of $\mathbf{n}_*$ and $\mathbf{s}_*$, we then may have

$$\alpha n_{x_*}s_{x_{**}} + \beta n_{y_*}s_{y_{**}} + n_{z_*}s_{z_{**}} = 0 \tag{67}$$

Similarly from the normality of $\mathbf{n}_*$ to $\mathbf{t}_*$ we have

$$\alpha n_{x_*}t_{x_{**}} + \beta n_{y_*}t_{y_{**}} + n_{z_*}t_{z_{**}} = 0 \tag{68}$$

Using Eqs. (67) and (68) in Eq. (64), Eq. (64) will be simplified to

$$\frac{\partial\varphi}{\partial n_*} = C\frac{\partial\varphi}{\partial n_{**}} \tag{69}$$

in which

$$C = \alpha n_{x_*}n_{x_{**}} + \beta n_{y_*}n_{y_{**}} + n_{z_*}n_{z_{**}} \tag{70}$$

Substituting values of n_{x_*} and n_{y_*} from Eq. (65) into Eq. (69) we will have

$$C = n_{z_*}/n_{z_{**}} \tag{71}$$

Since $\mathbf{n}_*$ and $\mathbf{n}_{**}$ are unit vectors we have

$$\begin{aligned}
n_{z_*} &= \left[1 + \left(\frac{n_{x_*}}{n_{z_*}}\right)^2 + \left(\frac{n_{y_*}}{n_{z_*}}\right)^2\right]^{-1/2}\\
n_{z_{**}} &= \left[1 + \left(\frac{n_{x_{**}}}{n_{z_{**}}}\right)^2 + \left(\frac{n_{y_{**}}}{n_{z_{**}}}\right)^2\right]^{-1/2}
\end{aligned} \tag{72}$$

Using Eq. (65) in Eq. (72) and doing some algebraic manipulations will give

$$C = \left[\left(\frac{n_{x_{**}}}{\alpha}\right)^2 + \left(\frac{n_{y_{**}}}{\beta}\right)^2 + n_{z_{**}}^2\right]^{-1/2} \tag{73}$$

Using Eqs. (69) and (73) in Eq. (53) we then finally have the formula for transformation of Neumann boundary condition as follows:

$$\frac{\partial\varphi}{\partial n} = \left[\left(\frac{n_{x_{**}}}{\alpha}\right)^2 + \left(\frac{n_{y_{**}}}{\beta}\right)^2 + n_{z_{**}}^2\right]^{-1/2}\frac{\partial\varphi}{\partial n_{**}}$$

Replacing α and β from Eqs. (55) and (56) will lead to

$$\frac{\partial\varphi}{\partial n} = \left[\frac{k_{x_*}}{k_{z_*}}n_{x_{**}}^2 + \frac{k_{y_*}}{k_{z_*}}n_{y_{**}}^2 + n_{z_{**}}^2\right]^{-1/2}\frac{\partial\varphi}{\partial n_{**}} \tag{74}$$

Eq. (74) gives us the transform and inverse transform of Neumann boundary conditions. It means that for using the direct transformation given in Eqs. (51) and (52) to transform the governing Eq. (5) to the Laplace Eq. (11), any Neumann boundary conditions $\partial\varphi/\partial n$ that are prescribed on the original domain should be transformed to $\partial\varphi/\partial n_{**}$ in the transformed domain by using Eq. (74). Thus it is clear that a preprocessing of the Neumann boundary conditions is needed. After solution of the Laplace equation in the transformed domain, any computed values of $\partial\varphi/\partial n_{**}$ should again be transformed to the original domain to find the $\partial\varphi/\partial n$ again with using Eq. (74). It means that a post processing for computed normal gradients is required after the Laplace equation has been solved.

5. BEM treatment of the transformed domain

The governing equation to be solved is given in Eq. (5) on the original domain Ω with boundary Γ. In the previous section we showed that we can use the transformation (51) to reach the transformed governing Eq. (11) in the transformed domain Ω_{**} with transformed boundary Γ_{**}. As it is very well established in the BEM literature for the Laplace equation, we then will have [3]

$$c_i\varphi_i+\int_{\Gamma_{**}} G\frac{\partial\varphi}{\partial n_{**}}d\Gamma=\int_{\Gamma_{**}}\varphi\frac{\partial G}{\partial n_{**}}d\Gamma \tag{75}$$

Here G is named as the Green's Function of and is equal to $1/4\pi r_{**}$ when the region is three-dimensional and the governing equation is the Laplace Equation and r_{**} is the distance from any point i to the integration point on the transformed boundary. c_i is between 0 and 1 and is equal to 1 if the point QUOTE i is inside the boundary, 1/2 if point QUOTE i is on a smooth boundary and is equal to zero when point QUOTE i is outside the boundary. If point QUOTE i is on a non-smooth part of the boundary (a boundary corner), $c_i$is equal to the special angle of the corner divided by 4π. The spatial angle _ is defined as the surface area of the sector of the unit sphere that is centered at the corner point x0 and lies inside the domain. The potential in any point in the domain can be calculated by Eq. (75), if both potential φ and its normal to boundary gradient $\partial\varphi/\partial n_{**}$ is given on the whole of the boundary. In well-posed problems, usually only one is prescribed by the boundary conditions. If φ is prescribed it can directly be used in (75) but if $\partial\varphi/\partial n$ is prescribed, $\partial\varphi/\partial n_{**}$ can be pre-calculated simply by Eq. (74). For calculating the potential anywhere in the domain, we need to calculate the unknown information on the boundary first i.e. we should calculate $\partial\varphi/\partial n_{**}$ on parts of the boundary that φ is prescribed and calculate on remaining parts of the boundary in which $\partial\varphi/\partial n_{**}$ is prescribed. To do this by BEM, we first discretize the boundary Γ_{**} to a finite number of surficial elements (in three-dimensional domains) each of finite number of nodes. Appropriate shape functions are defined for elements to enable us to interpolate the values of φ and $\partial\varphi/\partial n$ inside the element in terms of the nodal values. One can write Eq. (75) for each node on the boundary Γ_{**}. This will result in a set of simultaneous linear equations that can be solved for unknowns on the boundary. Completing the data on the boundary, one then can calculate the potential in any point in the domain by use of Eq. (75). If any $\partial\varphi/\partial n$ is needed to be calculated on parts of the boundary in which φ is prescribed, after calculating the , the calculated value can be used in Eq. (74) as the inverse transform of the Neumann boundary condition to calculate the . To see the detail formulations for the method, the reader is referenced to the previous publication of the authors [15]. A BEM code that was previously developed by authors for orthotropic media is developed for solving general anisotropic problems [15]. The evolution of the code includes the implementation of the presented direct transformation, transformed Neumann boundary conditions and transformed equilibrium equation. The code is called SEEPBEM3D. To have more information about the BEM treatment of the problem in the code, please refer to Rafiezadeh and Ataie-Ashtiani [15].

6. Transformation of equilibrium equation

When the physical model includes more than one type of material with different properties, usually the whole media is divided into sub-domains or sub-regions or zones in a manner that each domain is homogeneous by itself. Now consider a media made from m sub-domains that the sub-domains are homogeneous but have different hydraulic conductivity tensors $\mathbf{K}^{(m)}$. The sub-domains are connected with each other by interfaces between domains. Boundary conditions are provided for the boundary of the media but there is no information on the interfaces between sub-domains. Domain k and domain l are neighbor domains and domains k and l have $n^{(k)}$ and $n^{(l)}$ nodes respectively and there are n_I nodes on the interface between them. Eq. (75) can be written for each $n^{(k)}$ and $n^{(l)}$ nodes of domains k and l respectively, but as there is no data on the n_I nodes on the interface, two unknowns (φ and $\partial\varphi/\partial n_{**}$) for each node are added to the system of equations. To be able to solve the system of equations properly, two additional equations should be added to the system. These two equations are named compatibility and equilibrium equations.

Compatibility equation rules for continuity of the potential in the media and means that a physical point on the interface should have only one value for the potential, so for any point on the interface we will have

$$\varphi^{(k)}=\varphi^{(l)} \tag{76}$$

which the superscripts denote the domain index. Because after transformation, the potentials do not change, the Eq. (76) can directly be used after transformation of each domain.

The equilibrium equation calls for conservation of flowing mass between the domains, i.e. the normal to interface flowing mass that exits from one domain should enter to the adjacent domain, i.e.

$$\mathbf{q}^{(k)}.\mathbf{n}^{(k)}=-\mathbf{q}^{(l)}.\mathbf{n}^{(l)} \tag{77}$$

Applying Darcy's law we may have:

$$k_e^{(k)}\partial\varphi^{(k)}/\partial n^{(k)}=-k_e^{(l)}\partial\varphi^{(l)}/\partial n^{(l)} \tag{78}$$

which subscript e states for the equivalent hydraulic conductivity and the superscripts denote the domain index.

The transformation $\mathbf{T}$ that is calculated from Eq. (50) was a combination of a rotating transformation $\mathbf{q}$ and stretching transformation. In the rotating transformation, the coordinate axes rotate to be parallel to the principal axes of the hydraulic conductivity, i.e. k_{x_*}, k_{y_*} and k_{z_*} and therefore no deformation of domains' geometries occurs. However, in the stretching transformation the x- and y-coordinates are stretched in a manner that the equivalent hydraulic conductivities in the new stretched domain is equivalent to k_{z_*} and thus the governing equation is transformed to the Laplace equation and so the equivalent hydraulic conductivity in the transformed media is k_{z_*}. Thus the equilibrium Eq. (78) will become

$$k_{z_*}^{(k)}\partial\varphi^{(k)}/\partial n^{(k)}=-k_{z_*}^{(l)}\partial\varphi^{(l)}/\partial n^{(l)} \tag{79}$$

Substituting the transformed values of the normal gradients from Eq. (74) into Eq. (78) we then have

$$k_{z_*}^{(k)}\left[\frac{k_{x_*}^{(k)}}{k_{z_*}^{(k)}}n_{x_{**}}^{(k)^2}+\frac{k_{y_*}^{(k)}}{k_{z_*}^{(k)}}n_{y_{**}}^{(k)^2}+n_{z_{**}}^{(k)^2}\right]^{-1/2}\frac{\partial\varphi^{(k)}}{\partial n_{**}^{(k)}}=k_{z_*}^{(k)}\left[\frac{k_{x_*}^{(k)}}{k_{z_*}^{(k)}}n_{x_{**}}^{(k)^2}+\frac{k_{y_*}^{(k)}}{k_{z_*}^{(k)}}n_{y_{**}}^{(k)^2}+n_{z_{**}}^{(k)^2}\right]^{-1/2}\frac{\partial\varphi^{(k)}}{\partial n_{**}^{(k)}} \tag{80}$$

Eq. (80) is the transformed equilibrium equation. Using the two compatibility Eq. (76) and equilibrium Eq. (80), two additional equations for each node on the interface is provided and the simultaneous global system of equations can be solved. Assembling the system of equation of each sub-domain into a global system of equations can then be performed as it is done in any other standard multi-domain BEM and therefore is not covered here, but one can refer to Rafiezadeh and Ataie-Ashtiani [15] for more explanations Fig. 2 provides a schematic for visual comprehension of the transformations. A model containing four

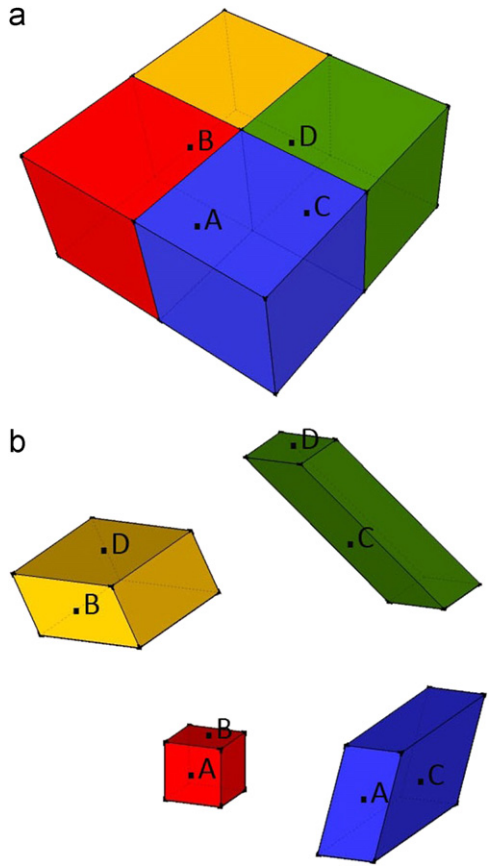

Fig. 2. (a) Physical model containing four sub-domains, (b) distorted (transformed) model after transformation. (For interpretation of the references to color in this figure, the reader is referred to the web version of this article.)

sub-domains (blue, red, green and yellow) is shown in this schematic. Typical nodes on the interfaces between domains are also depicted. A is a node on the interface between blue and red, B is a node on the interface between red and yellow, C is a node on the interface between blue and green and D is a node on the interface between green and yellow subdomains. Each subdomain has a different hydraulic conductivity tensor. As shown in the depiction, because of different permeability tensor each subdomain undergoes a different transformation and distortion. The distorted subdomains may have gaps and overlaps. These gaps and overlaps do not have any effect in the solution of the problem as system of equations for each subdomain is independent from the other ones. Compatibility and equilibrium conditions for the nodes on the interfaces can then make connections between the system of equations of each domain and make the global system of equations. For example for node *C*, the compatibility equation is $\varphi^{(b)}=\varphi^{(g)}$ and the equilibrium equation is

$$k_{z_*}^{(b)}\left[\frac{k_{x_*}^{(b)}}{k_{z_*}^{(b)}}n_{x_{**}}^{(b)^2}+\frac{k_{y_*}^{(b)}}{k_{z_*}^{(b)}}n_{y_{**}}^{(b)^2}+n_{z_{**}}^{(b)^2}\right]^{-1/2}\frac{\partial\varphi^{(b)}}{\partial n_{**}^{(b)}}=k_{z_*}^{(g)}\left[\frac{k_{x_*}^{(g)}}{k_{z_*}^{(g)}}n_{x_{**}}^{(g)^2}+\frac{k_{y_*}^{(g)}}{k_{z_*}^{(g)}}n_{y_{**}}^{(g)^2}+n_{z_{**}}^{(g)^2}\right]^{-1/2}\frac{\partial\varphi^{(g)}}{\partial n_{**}^{(g)}}$$

Similar equations can be written for any nodes on the interfaces between two zones. In case when multiple zones with distinct hydraulic conductivities are joined together and share one point as intersection point (for example the nodes on the line connecting the four subdomains in the depiction), a singularity happens at the intersection point. From a practical point of view, in most calculations the intersection point is simply avoided, but additional nodes are taken on each of the inter-zonal boundaries close to the intersection. The results may not be entirely accurate very close to the intersection but are usually more than accurate enough for practical purposes [5].

7. Interior solutions

Solution of the Laplace equation of the transformed domain may give us the potential and its gradients in any point in the domain, i.e. we may have φ, $\partial\varphi/\partial x_{**}$, $\partial\varphi/\partial y_{**}$ and $\partial\varphi/\partial z_{**}$. Potential is the same on the distorted and the physical domains, but we need an inverse transformation for the gradients to have $\partial\varphi/\partial x$, $\partial\varphi/\partial y$ and $\partial\varphi/\partial z$ on the physical domain. Using the chain rule, we have

$$\begin{aligned}
\frac{\partial\varphi}{\partial x}&=\frac{\partial\varphi}{\partial x_{**}}\frac{\partial x_{**}}{\partial x}+\frac{\partial\varphi}{\partial y_{**}}\frac{\partial y_{**}}{\partial x}+\frac{\partial\varphi}{\partial z_{**}}\frac{\partial z_{**}}{\partial x}\\
\frac{\partial\varphi}{\partial y}&=\frac{\partial\varphi}{\partial x_{**}}\frac{\partial x_{**}}{\partial y}+\frac{\partial\varphi}{\partial y_{**}}\frac{\partial y_{**}}{\partial y}+\frac{\partial\varphi}{\partial z_{**}}\frac{\partial z_{**}}{\partial y}\\
\frac{\partial\varphi}{\partial z}&=\frac{\partial\varphi}{\partial x_{**}}\frac{\partial x_{**}}{\partial z}+\frac{\partial\varphi}{\partial y_{**}}\frac{\partial y_{**}}{\partial z}+\frac{\partial\varphi}{\partial z_{**}}\frac{\partial z_{**}}{\partial z}
\end{aligned}\tag{81}$$

From Eqs. (51) and (52) we have

$$\begin{aligned}
\frac{\partial x_{**}}{\partial x}&=(k_{z_*}/k_{x_*})^{\frac{1}{2}}V_{1x}\\
\frac{\partial x_{**}}{\partial y}&=(k_{z_*}/k_{x_*})^{\frac{1}{2}}V_{1y}\\
\frac{\partial x_{**}}{\partial z}&=(k_{z_*}/k_{x_*})^{\frac{1}{2}}V_{1z}\\
\frac{\partial y_{**}}{\partial x}&=(k_{z_*}/k_{y_*})^{\frac{1}{2}}V_{2x}\\
\frac{\partial y_{**}}{\partial y}&=(k_{z_*}/k_{y_*})^{\frac{1}{2}}V_{2y}\\
\frac{\partial y_{**}}{\partial z}&=(k_{z_*}/k_{y_*})^{\frac{1}{2}}V_{2z}\\
\frac{\partial z_{**}}{\partial x}&=V_{3x}\\
\frac{\partial z_{**}}{\partial y}&=V_{3y}\\
\frac{\partial z_{**}}{\partial z}&=V_{3z}
\end{aligned}\tag{82}$$

Substituting the derivatives from Eq. (82) into Eq. (81), we will have

$$\begin{aligned}
\frac{\partial\varphi}{\partial x}&=(k_{z_*}/k_{x_*})^{\frac{1}{2}}V_{1x}\frac{\partial\varphi}{\partial x_{**}}+(k_{z_*}/k_{y_*})^{\frac{1}{2}}V_{2x}\frac{\partial\varphi}{\partial y_{**}}+V_{3x}\frac{\partial\varphi}{\partial z_{**}}\\
\frac{\partial\varphi}{\partial y}&=(k_{z_*}/k_{x_*})^{\frac{1}{2}}V_{1y}\frac{\partial\varphi}{\partial x_{**}}+(k_{z_*}/k_{y_*})^{\frac{1}{2}}V_{2y}\frac{\partial\varphi}{\partial y_{**}}+V_{3y}\frac{\partial\varphi}{\partial z_{**}}\\
\frac{\partial\varphi}{\partial z}&=(k_{z_*}/k_{x_*})^{\frac{1}{2}}V_{1z}\frac{\partial\varphi}{\partial x_{**}}+(k_{z_*}/k_{y_*})^{\frac{1}{2}}V_{2z}\frac{\partial\varphi}{\partial y_{**}}+V_{3z}\frac{\partial\varphi}{\partial z_{**}}
\end{aligned}\tag{83}$$

Eq. (83) present the inverse transformation for calculating the gradients in the interior points of the physical domain in terms of the values of the gradients in the transformed domain which were calculated by BEM. Writing Eq. (83) in the matrix notation, we have

$$\mathbf{q}=\mathbf{T}^T\mathbf{q}_{**}\tag{84}$$

8. Verification examples

To examine the present formulations for the domain transformation, Neumann boundary condition transformation and the transformed equilibrium equation, three examples are considered. All of the examples include general anisotropic cases. The examples are solved by SEEPBEM3D and the results are compared with FEM simulation results using the ANSYS software. To solve a seepage problem in a general anisotropic media with this finite element software we have used the analogy between seepage and

heat conduction. The governing equation of seepage and heat transfer in a general anisotropic media is analogous. In the governing equation of heat conduction, the tensor of thermal conduction replaces the hydraulic conductivity in seepage and the temperature replaces the potential head.

The first example studies the head distribution around a constant-head pumping well drilled in an anisotropic media and is a single-domain problem. This example shows the accuracy of the direct transformation. In the second example, a pumping well in a two-layer anisotropic media is considered. The aquifer has two domains to check the accuracy of the transformed Neumann and equilibrium equations. The third example is to model the seepage through foundation of a gravity dam placed in a V-shaped valley folded from an anisotropic layer of sedimentations. This example contains two general anisotropic domains.

8.1. Well in anisotropic media

A well of 1.0 m radius is drilled into a confined aquifer of 10 m depth. The aquifer is made of a layer of anisotropic materials. The hydraulic conductivity of the aquifer is defined by a fully populated tensor

$$K = \begin{bmatrix} 7.8206 & 0.3990 & 2.1061 \\ 0.3990 & 6.6206 & 0.6364 \\ 2.1061 & 0.6364 & 9.8588 \end{bmatrix} \times 10^{-5}\ m/\mathrm{sec}$$

The aquifer is assumed to be a cylinder of 100 m radius that the well is drilled in its axis. The sketch of the model is given in Fig. 3. Total head of the aquifer is 30 m and in the well the potential head is equal to 15 m. The aquifer is a confined one and no flow is possible from top and bottom borders of the aquifer. Based on the definition of the problem, boundary conditions for the model are given in Table 1.

To model the geometry with BEM, the boundaries are discretized by triangular linear elements. A BEM mesh of the model is given in Fig. 4. The BEM mesh includes one domain, 1024 nodes and 2048 elements. After applying the direct domain transformation to the problem, the geometry of the model will distort and the distorted BEM mesh of the problem after transformation in

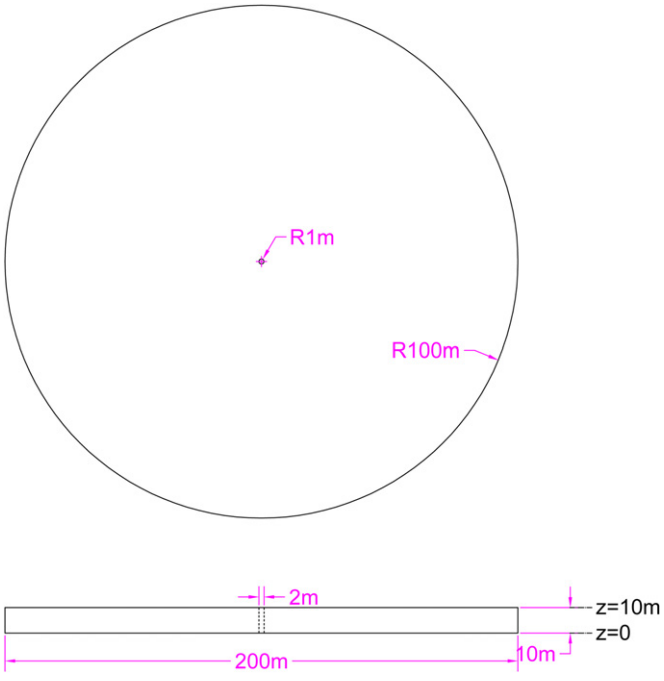

Fig. 3. Sketch of model in example 1.

Table 1
Boundary conditions of example 1.

Face	Boundary condition
Aquifer top ($z=10$ m)	$\partial\varphi/\partial n=0$
Aquifer bottom ($z=0$)	$\partial\varphi/\partial n=0$
Aquifer out ring ($x^2+y^2=100^2$)	$\varphi=30$ m
Well wall ($x^2+y^2=1$)	$\varphi=15$ m

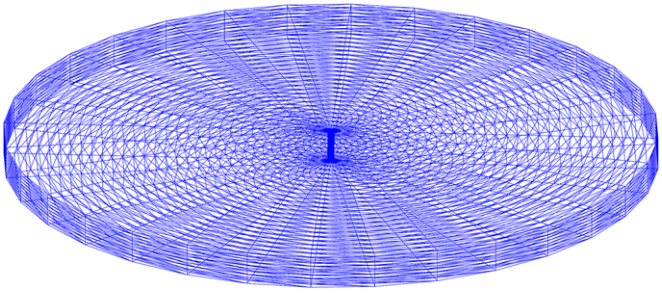

Fig. 4. BEM mesh for example 1.

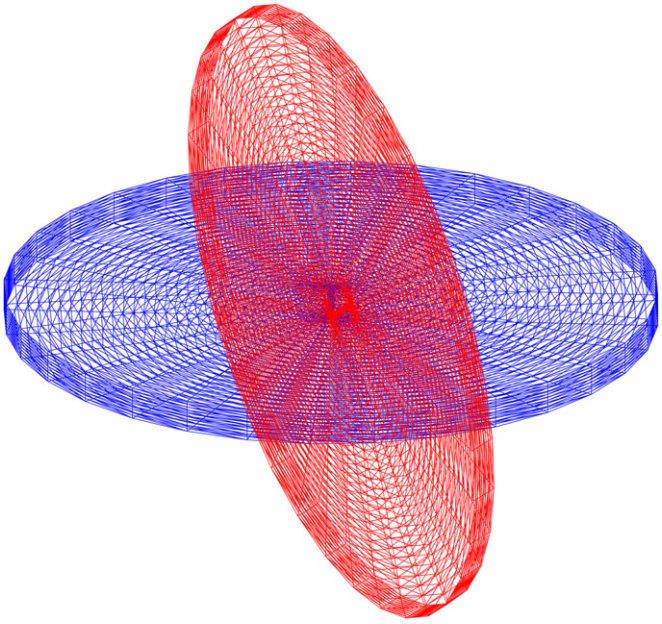

Fig. 5. Distorted model mesh (red) after transformation and original model mesh (blue). (For interpretation of the references to color in this figure legend, the reader is referred to the web version of this article.)

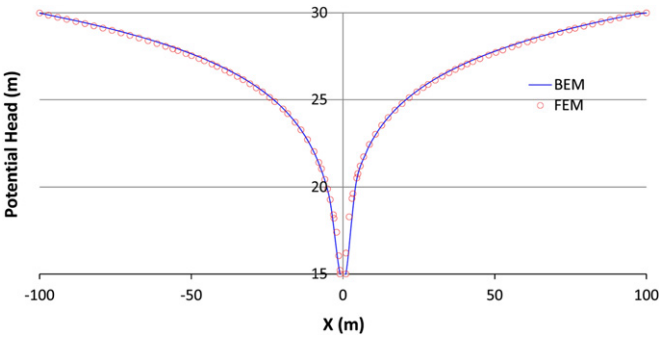

Fig. 6. Potential head along y-axis on the bottom of aquifer.

which the Laplace equation governs is shown in Fig. 5. The distorted model was solved with standard BEM for Laplace equation. To verify the accuracy and correctness of the proposed transformation, the problem was also solved by the finite element method. The calculated potential head of the aquifer on the bottom boundary along the line x-axis ($y=0$) is plotted in Fig. 6. In this figure one can compare the calculated results of BEM with FEM. The FEM model includes 363,165 nodes and 326,940 hexahedral elements. Excellent agreement of the results of BEM and FEM shows the veracity of the proposed transformation. To show the effect of the cross-diagonal terms of the hydraulic conductivity tensor, the model also has been run in orthotropic case in which the cross-diagonal terms of the conductivity tensor have been set to zero. A comparison of the normal to boundary gradients at the well wall on mid-height of the well is shown in Fig. 7 for the general anisotropic and orthotropic cases.

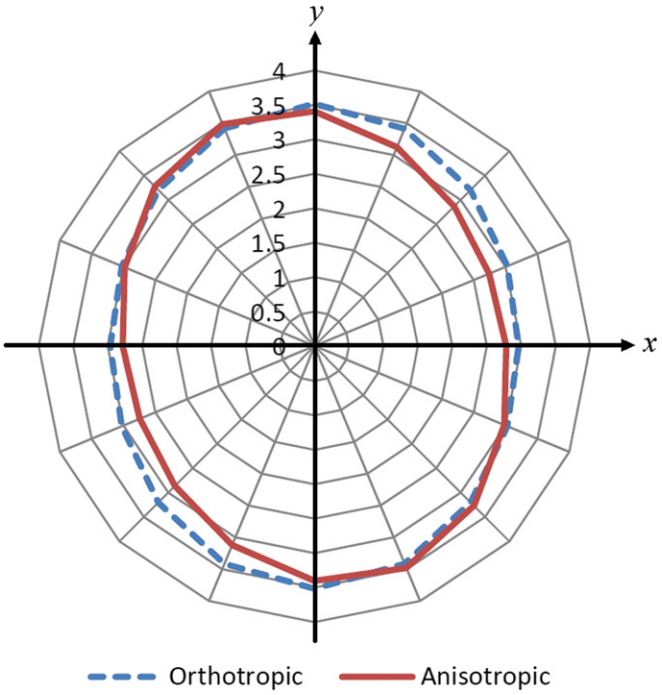

Fig. 7. Comparison of normal to boundary gradients at the well wall ($x^2+y^2=1$) on $z=5$ m in orthotropic and general anisotropic cases.

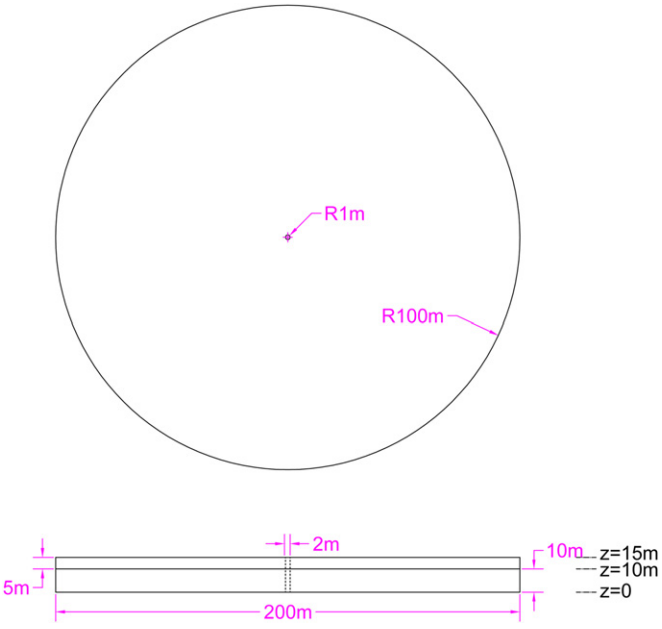

Fig. 8. Sketch of model of example 2.

8.2. Well in layered anisotropic media

A well of 1.0 m radius is considered in a confined aquifer of 15 m depth. The aquifer is a layered aquifer with two layers of

Table 2
Boundary conditions of example 2.

Face	Boundary condition
Top layer	
Aquifer top ($z=15$ m)	$\partial\varphi/\partial n=0$
Layer bottom ($z=10$ m)	Interface conditions
Aquifer out ring ($x^2+y^2=100^2$)	$\varphi=30$ m
Well wall ($x^2+y^2=1$)	$\varphi=15$ m
Bottom layer	
Layer top ($z=10$ m)	Interface conditions
Aquifer bottom ($z=0$)	$\partial\varphi/\partial n=0$
Aquifer out ring ($x^2+y^2=100^2$)	$\varphi=30$ m
Well wall ($x^2+y^2=1$)	$\varphi=15$ m

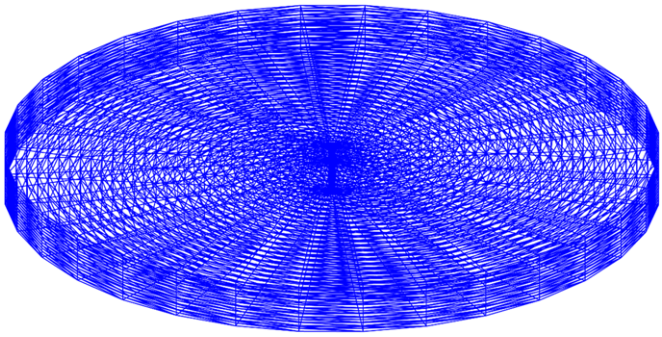

Fig. 9. BEM mesh of example 2.

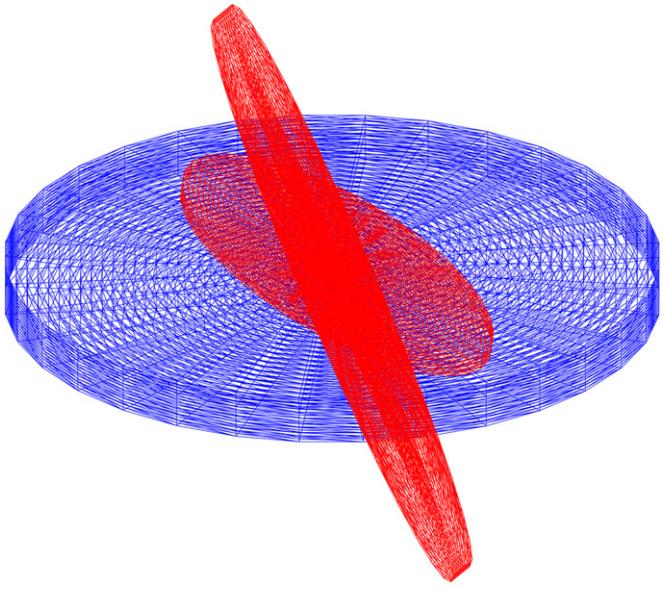

Fig. 10. Distorted mesh of the model (red) with original model mesh (bue). (For interpretation of the references to color in this figure legend, the reader is referred to the web version of this article.)

different hydraulic conductivities. Both of layers are anisotropic. The top layer is of 5 m depth and the bottom layer has 10 m depth. The hydraulic conductivity tensor of the top layer is

$$\mathbf{K}_{top} = \begin{bmatrix} 30 & 3 & 2 \\ 3 & 33 & 6 \\ 2 & 6 & 10 \end{bmatrix} \times 10^{-5}\ m/\text{sec}$$

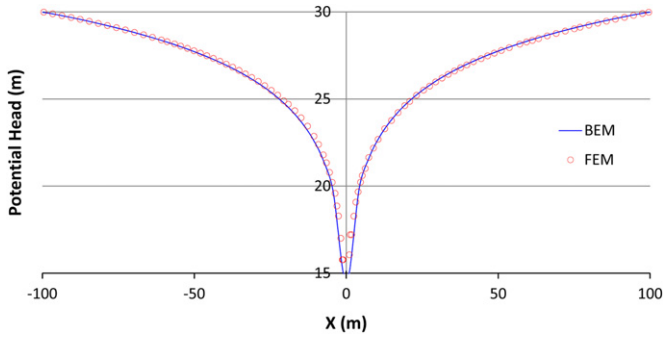

Fig. 11. Potential head along $y=0$ on the interface between two layers.

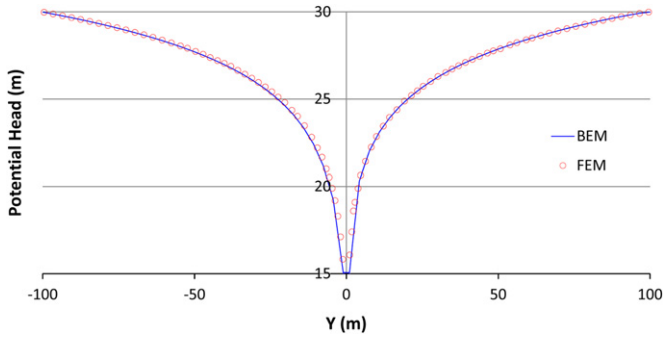

Fig. 12. Potential head along $x=0$ on the interface between two layers.

The hydraulic conductivity tensor of the bottom layer is

$$\mathbf{K}_{bottom} = \begin{bmatrix} 7 & 0.4 & 2 \\ 0.4 & 6 & 2 \\ 2 & 2 & 9 \end{bmatrix} \times 10^{-5}\ m/\text{sec}$$

The aquifer is assumed to be a cylinder of 100 m radius that the well is drilled in its axis. The sketch of the model is given in Fig. 8. Total head of the aquifer is 30 m and in the well the potential head is equal to 15 m. The aquifer is a confined one and no flow is possible from top and bottom borders of the aquifer. Based on the definition of the problem, boundary conditions for the model are given in Table 2.

To model the geometry with BEM, the boundaries are discretized by triangular linear elements. A BEM mesh of the model is given in Fig. 9. The BEM mesh includes two domains (top and bottom domains), 5056 nodes and 10,112 elements. After applying the direct domain transformation to the problem, the geometry of the model will distort and the distorted BEM mesh of the problem after transformation in which the Laplace equation governs is shown in Fig. 10. As it is clear in the figure, because of different hydraulic conductivity tensors of the two domains, the after-transformation distortion of the domains are also different. The distorted model was solved with standard BEM for Laplace equation. To verify the accuracy and correctness of the proposed transformation, the problem was also solved by the finite element method. The calculated potential heads of the aquifer interface of the two domains along the line x-axis ($y=0$) and y-axis ($x=0$) are plotted in Fig. 11 and Fig. 12, respectively. In these figures one can compare the calculated results of BEM with FEM. The FEM model includes 528,144 nodes and 163,460 hexahedral elements. Again, the excellent agreement of the BEM and FEM results shows the veracity of the proposed transformation and the formulas given for transformation of equilibrium equation for multi-domain general anisotropic media.. To show the effect of the cross-diagonal terms of the hydraulic conductivity tensors, the model also has been run in orthotropic case in which the cross-diagonal terms of both conductivity tensors have been set to zero. A comparison of the normal to boundary gradients at the well wall on different elevations of the well is shown in Fig. 13 for the general anisotropic and orthotropic cases.

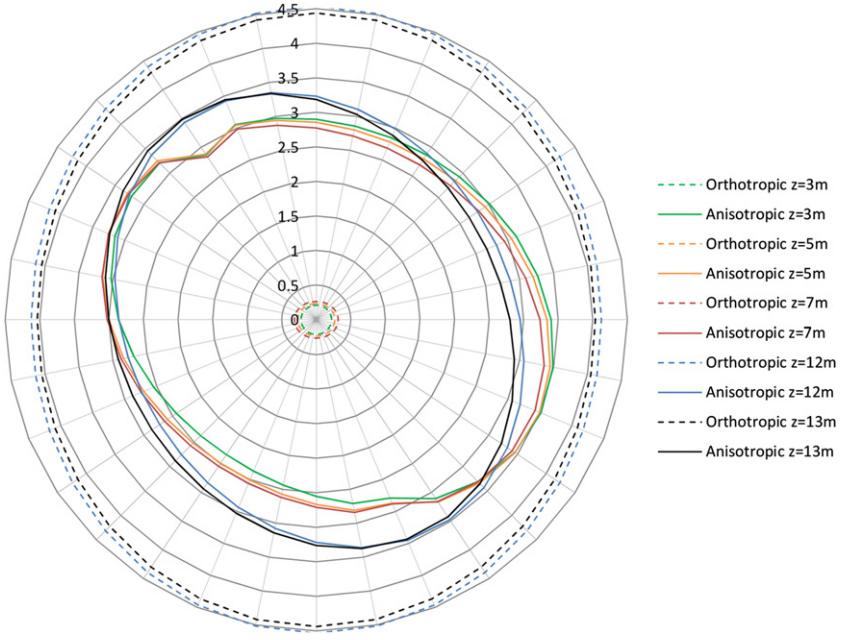

Fig. 13. Comparison of normal to boundary gradients at the well wall ($x^2+y^2=1$) on different elevations in orthotropic and general anisotropic cases.

8.3. Dam on a V-shaped anisotropic valley

In third example, the seepage flow across the foundation and banks of a gravity dam is solved. It has been shown in [32] that when seepage through dam foundation happens and when the banks of the river are permeable, two-dimensional approximation is not a good approximation and three-dimensional analysis should be performed. A three-dimensional sketch of the problem is shown in Fig. 14. The gravity dam is founded on a V-shaped valley. The foundation is made from a folded sedimentary layer of rock that is situated on a horizontal thick layer of igneous rock. The sedimentary layer is permeable and anisotropic, while the igneous rock is almost impermeable and is assumed as the bedrock.

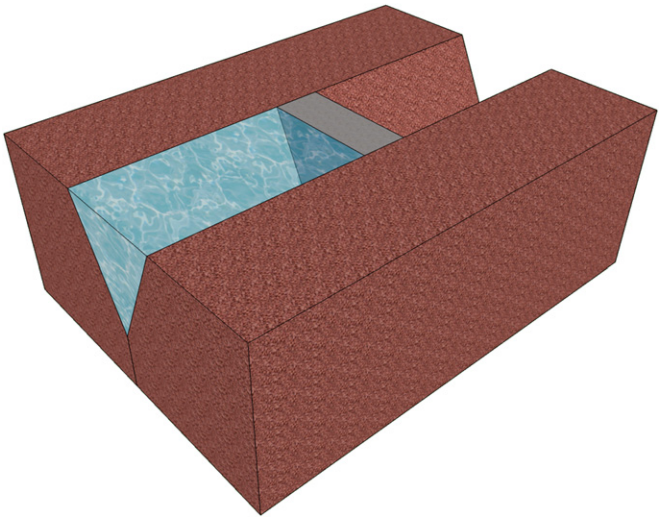

Fig. 14. Three-dimensional sketch of example 3.

The hinge line of the geological fold is parallel to the river axis and the inter-limb angle of the fold is about 53°. Height of dam is 100 m and the dam crest length is 100 m. Datum is taken at the bedrock and the thickness of the foundation on the river axis is equal to 50 m. Standing at the river axis and looking at downstream, the block of the sedimentary rock at the left is called the left-side foundation and the block of the sedimentary rock at the right is called the right-side foundation. A sketch of the problem is given in Fig. 15. Because the sedimentary rock layer is folded, the elements of the hydraulic conductivity tensor in the left-side and right-side foundations are not equal and thus there is a double-domain seepage media for modeling. The hydraulic conductivity tensor of the left-side foundation is

$$\mathbf{K}_{left} = \begin{bmatrix} 20 & 0.01 & 0.01 \\ 0.01 & 2.8 & -3.6 \\ 0.01 & -3.6 & 8.2 \end{bmatrix} \times 10^{-5}\ m/\text{sec}$$

And the hydraulic conductivity tensor of the right-side foundation is

$$\mathbf{K}_{right} = \begin{bmatrix} 20 & 0.01 & 0.01 \\ 0.01 & 2.8 & 3.6 \\ 0.01 & 3.6 & 8.2 \end{bmatrix} \times 10^{-5}\ m/\text{sec}$$

Length of the foundation in the model has been taken 400 m. Water pressure head of the river is 150 m in the upstream and 50 m in the downstream. Based on the definition of the problem, boundary conditions for the model are given in Table 3.

To model the geometry with BEM, the boundaries are discretized by triangular linear elements. A BEM mesh of the model is given in Fig. 16. The BEM mesh includes two domains (top and bottom domains), 4020 nodes and 8032 elements. After applying the direct domain transformation to the problem, the geometry of the model will distort and the distorted BEM mesh of the problem after transformation in which the Laplace equation governs is shown in Fig. 17. As it is clear in the figure, because of different

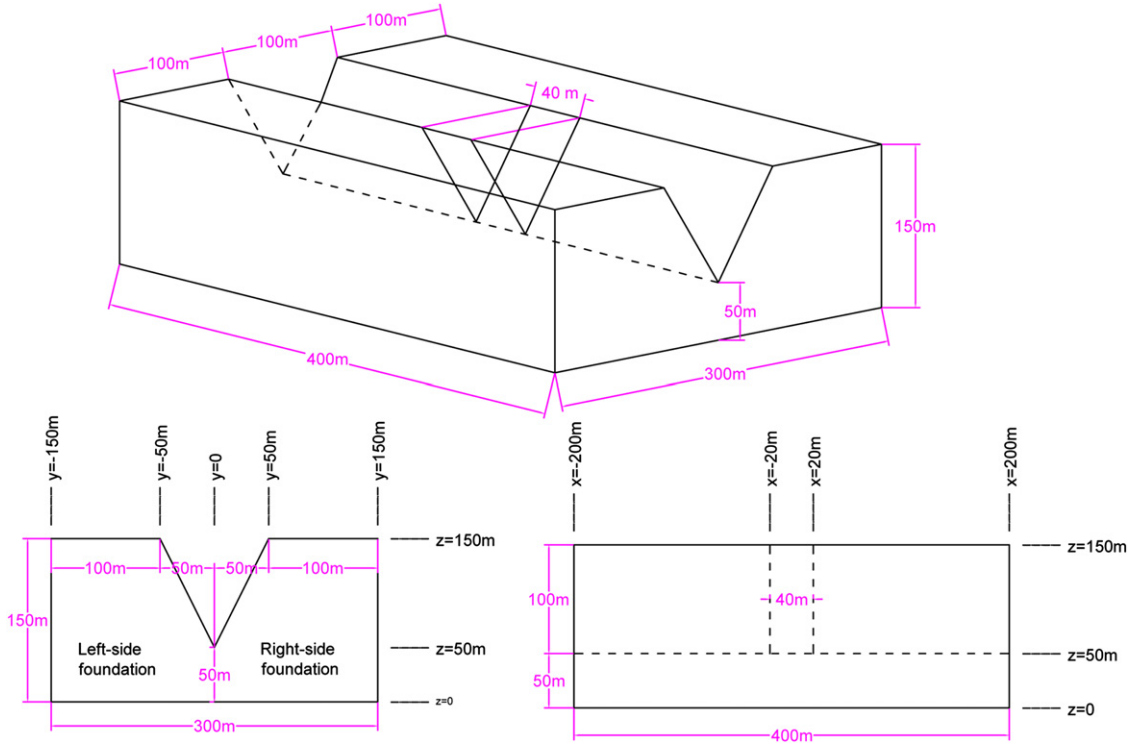

Fig. 15. Sketch of model in example 3.

Table 3
Boundary conditions of example 3.

Face	Boundary condition
Left-side foundation	
Upstream end ($x=-200$ m)	$\varphi=150$ m
Downstream end ($x=200$ m)	$\varphi=50$ m
River axis plane ($y=0$)	Interface conditions
Left end ($y=-150$ m)	$\partial\varphi/\partial n=0$
Upstream river bed ($z+2y=50$ m), (-200 m $< x <$ -20 m)	$\varphi=150$ m
Downstream river bed ($z+2y=50$ m), (20 m $< x <$ 200 m)	$\varphi=50$ m
Below dam ($z+2y=50$ m), (-20 m $< x <$ 20 m)	$\partial\varphi/\partial n=0$
Bed rock ($z=0$)	$\partial\varphi/\partial n=0$
Right-side foundation	
Upstream end ($x=-200$ m)	$\varphi=150$ m
Downstream end ($x=200$ m)	$\varphi=50$ m
River axis plane ($y=0$)	Interface conditions
Right end ($y=150$ m)	$\partial\varphi/\partial n=0$
Upstream river bed ($z-2y=50$ m), (-200 m $< x <$ -20 m)	$\varphi=150$ m
Downstream river bed ($z-2y=50$ m), (20 m $< x <$ 200 m)	$\varphi=50$ m
Below dam ($z-2y=50$ m), (-20 m $< x <$ 20 m)	$\partial\varphi/\partial n=0$
Bed rock ($z=0$)	$\partial\varphi/\partial n=0$

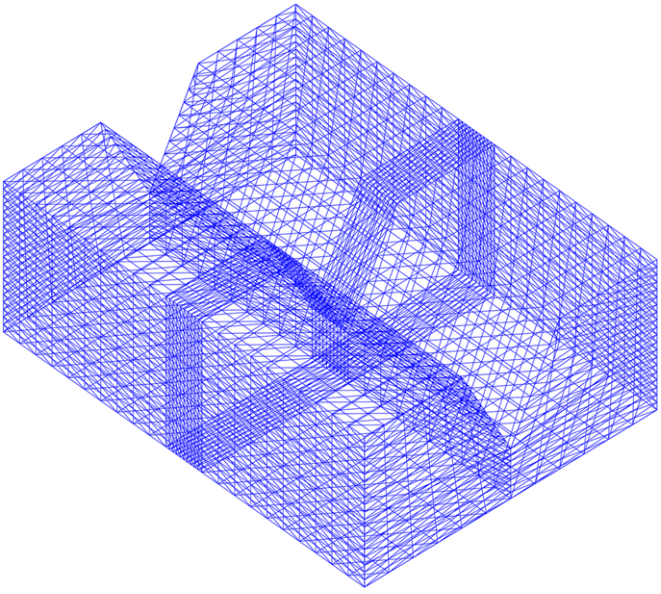

Fig. 16. BEM mesh of example 3.

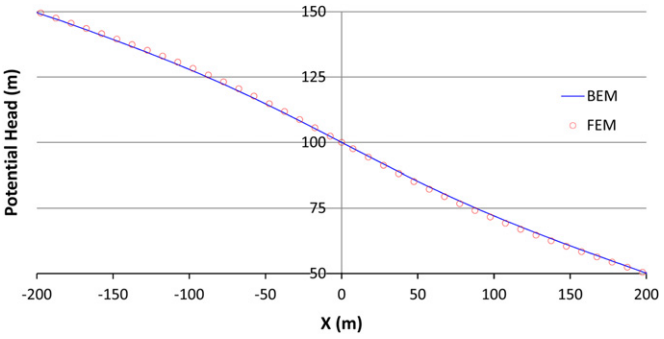

Fig. 18. Potential head along $y=0$ on the bed rock.

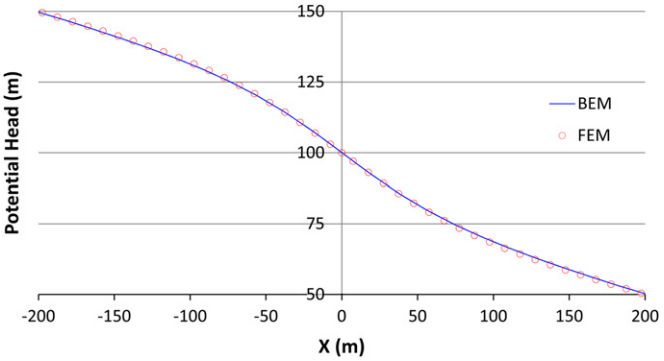

Fig. 19. Potential head along $y=0$, $z=25$ m.

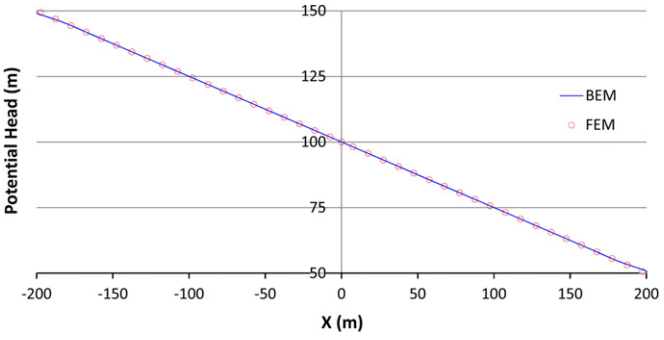

Fig. 20. Potential head along $y=150$ m on the bed rock.

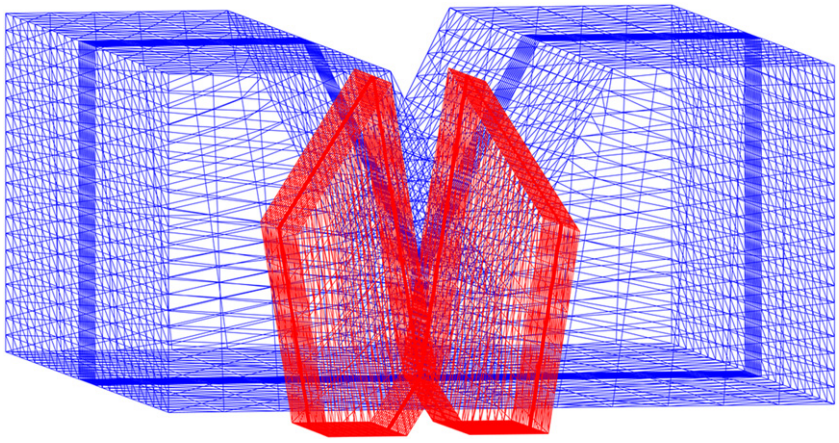

Fig. 17. Distorted mesh (red) with the original mesh (blue). (For interpretation of the references to color in this figure legend, the reader is referred to the web version of this article.)

hydraulic conductivity tensors of the two domains, the after-transformation distortion of the domains are also different. The distorted model was solved with standard BEM for Laplace equation. To verify the accuracy and correctness of the proposed transformation, the problem was also solved by the finite element method. The FEM model includes 229,955 nodes and 107,520 hexahedral elements. The calculated potential heads along the x-axis ($y=0$) on the bed rock is plotted in Fig. 18. A comparison of the potential head by FEM and BEM on the line $y=0$, $z=25$ on the interface between the two domains is depicted in Fig. 19. In Fig. 20 the calculated potential head along the line $y=150$, $z=0$ is given. Once again, excellent agreement of the BEM and FEM solutions is observed. Contours of the potential head on the bed rock and the interface between the two domains in the river axis are shown in Fig. 21 for two cases of anisotropic and orthotropic materials. In the orthotropic case we have set the cross-permeability terms zero to give a comparison on the results of the two cases and the importance of cross-diagonal terms in the conductivity tensor. A comparison of gradients has also been shown in Fig. 22 along a horizontal line on $z=75$ m and $z=50$ m.

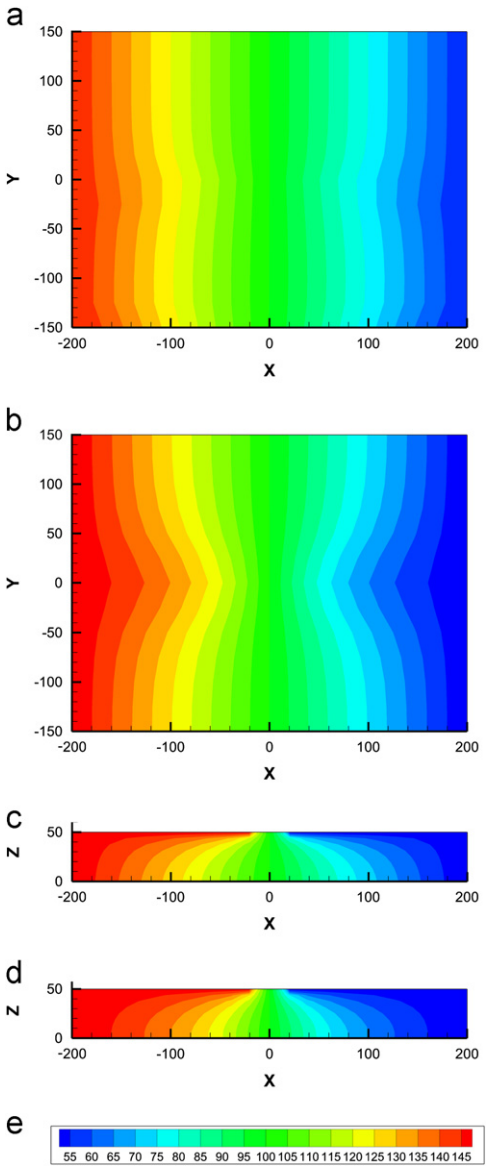

Fig. 21. Potential head contours (a) on bed rock ($z=0$) anisotropic, (b) on bed-rock ($z-0$) orthotropic, (c) on the river axis plane ($y=0$) anisotropic, (d) on the river axis plane ($y=0$) orthotropic, (e) Legend.

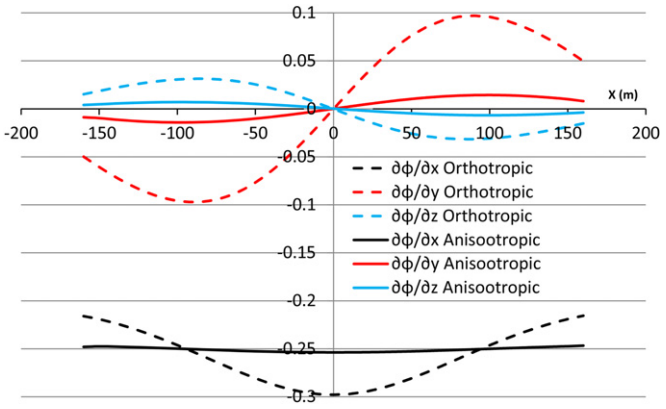

Fig. 22. Comparison of gradients in general anisotropic and orthotropic cases on $y=75$ m, $z=50$ m.

9. Conclusions

General anisotropic materials are very common when dealing with seepage problems especially on dam-sites where dams are founded on rivers in valleys and supplying water from aquifers by means of digging wells. Heterogeneities are also very common because usually dam-sites and aquifers are made of sedimentary materials which are deposited in layers of different hydraulic properties. These heterogeneities are usually dealt by different sub-domains of different hydraulic properties. The authors had previously developed a BEM solution for seepage analysis in a specific class of anisotropic problems (i.e. orthotropic problems) which the cross-diagonal elements of the hydraulic conductivity tensors vanish. This paper is an extension to the previous work and generalizes the problem to the general anisotropic materials. Using the analytical eigenvalues and eigenvectors and combining with the stretching transformation which had been presented in [15], a new transformation has been developed in this paper that transforms the general anisotropic governing equation to the Laplace equation. Using this transformation needs also transforming the flux boundary conditions and equilibrium equations and thus the formulas for transforming the Neumann boundary conditions and equilibrium equations have been provided in this paper, accordingly.

Advantages of the present model can be mentioned as following:

- The study of round-off error is crucial when solving a linear system of equations, since it may pollute and even destroy the solution of the problem[33]. The accumulation of round-off errors in models with relatively large number of nodes in finite-element models versus relatively few nodes in boundary-element models is an advantage for BEM solutions. Previous researches have shown that matrix inversion and processes, and algebraic computations are prone to accumulation of round-off errors when there are heavy meshes and the matrix sizes are very large [34–37].
- The transformation approach presented will transform the governing equation to the Laplace equation, and thus any BEM code for potential problems can be simply used.
- The transformation method only needs some very simple coding due to preprocessing of the geometry and Neumann boundary conditions and post processing the solved flux results, so not much effort is needed to expand a standard BEM code for Laplace equation to the general anisotropic seepage analysis code.

- Developing the inter-zonal equilibrium equations in three-dimensions lets the true coupling of the neighbor anisotropic domains in multi-domain problems.

We have solved several examples of general anisotropic multi-domain seepage problems that are frequently arisen in the engineering practice. We have verified our results with 3D FEM models and showed that the results are accurate. Examples can illustrate the simplicity of the model and the accuracy of the proposed scheme.

References

[1] Cheng AH-D, Cheng D. Heritage and early history of the boundary element method. Eng Anal Boundary Elem 2005;29:268–302.
[2] Belytschko T, Lu Y, Gu L. Element-free Galerkin methods. Int J Numer Meth Eng 1994;37:229–56.
[3] Brebbia C. The boundary element method for engineers. London: Pentech Press; 1978.
[4] Das B. Advanced soil mechanics. NewYork: McGraw-Hill Book Company; 1990.
[5] Liggett J, Liu P-F. The boundary integral equation method for porous media flow. London: George Allen & Unwin (Publishers) Ltd.; 1983.
[6] Read W, Volker R. BIEM/QLS computer generated solutions for sloping base seepage problems. Comput Fluids 1994;23:115–24.
[7] Brebbia C, Chang O. Boundary elements applied to seepage problems in zoned anisotropic soils. Adv Eng Software 1979;1(3):95–105.
[8] Mera M, Elliott L, Ingham D, Lesnic D. A comparison of boundary element method formulations for steady state anisotropic heat conduction problems. Eng Anal Boundary Elem 2001;25:115–28.
[9] Rungamornrat J, Wheeler M. Weakly singular integral equations for Darcy's flow in anisotropic porous media. Eng Anal Boundary Elem 2006;30:237–46.
[10] Rungamornrat J. Modeling of flow in three-dimensional, multizone, anisotropic porous media with weakly singular integral equation method. J Eng Mech, ASCE 2009:828–38.
[11] Chugh A, Falvey H. A computer program for planar seepage analysis in a zoned anisotropic medium by the boundary element method. Adv Eng Software 1983;5:196–201.
[12] Chugh A, Falvey H. Seepage analysis in a zoned anisotropic medium by the noundary element method. Int J Numer Anal Methods Geomech 1984: 399–407.
[13] Chugh A. Flow nets for zoned anisotropic media by the boundary element method. Comput Struct 1988;29:207–20.
[14] Laef O, Liggett J, Liu P-F. BIEM solutions to combinations of leaky, layered, confined, unconfined, nonisotropic aquifers. Water Resour Res 1981;17: 1431–44.
[15] Rafiezadeh K, Ataie-Ashtiani B. Three dimensional flow in anisotropic zoned porous media using boundary element method. Eng Anal Boundary Elem 2012;36:812–24.
[16] Viesmann J, Lewis G. Introduction to hydrology. New York: Harper Collins College Publishers; 1996.
[17] Zhang Y, Liu Z, Chen J, Gu Y. A novel boundary element approach for solving the anisotropic potential problems. Eng Anal Boundary Elem 2011;35: 1181–9.
[18] Marczak R, M D. Alternative forms of fundamental solutions for 3-D anisotropic heat transfer, Buenos Aires. Mec Computl 2010;XXIX:5639–54.
[19] Marczak R, Mitsunori D. New derivations of the fundamental solution for heat conduction problems in three-dimensional general anisotropic media. Int J Heat Mass Transfer 2011;54:3605–12.
[20] Shiah Y, Tan C. BEM treatment of two-dimensional anisotropic field problems by direct domain mapping. Eng Anal Boundary Elem 1997;20:347–51.
[21] Hsieh M, Ma C. Analytical investigations for heat conduction problems in anisotropic thin-layer media with embedded heat sources. Int J Heat Mass Transfer 2002;45:4117–32.
[22] Ma C, Chang S. Analytical exact solutions of heat conduction problems for anisotropic multi-layered media. Int J Heat Mass Transfer 2004;47:1643–55.
[23] Shiah Y, Tan C. BEM treatment of three-dimensional anisotropic field problems by direct domain mapping. Eng Anal Boundary Elem 2004;28: 43–52.
[24] Shiah Y, Hwang P-W, R-B Y. Heat conduction in multiply adjoined anisotropic media with embedded point heat sources. J Heat Transfer 2006;128:207–14.
[25] Maidment D. Handbook of hydrology. New York: McGraw-Hill Inc.; 1993.
[26] Hsieh P, Neuman S. Field determination of the threedimensional hydraulic conductivity tensor of anisotropic media, 1, theory. Water Resour Res 1985;21(11):1655–65.
[27] Hsieh P, Neuman S, Stiles G, Simpson E. Field determination of the three-dimensional hydraulic conductivity tensor of anisotropic media, 2, methodology and application to fractured rocks. Water Resour Res 1985;21(1): 1667–76.
[28] Wang M, Kulatilake P, Um J, Narvaiz J. Estimation of REV size and three-dimensional hydraulic conductivity tensor for a fractured rock mass through a single well packer test and discrete fracture fluid flow modeling. Int J Rock Mech Min Sci 2002;39:887–904.
[29] Kreyszig E. Advanced engineering mathematics. New York/London: John Wiley & Sons, Inc.; 2006.
[30] Hasan K, Basser P, Parker D, Alexander A. Analytical computation of the Eigenvalues and Eigenvectors in DT-MRI. J Magn Reson 2001;39:887–904.
[31] Borisenko A, Tarapov I. Vector and Tensor Analysis with Applications. New York: Dover; 1968 pp. 121–122.
[32] Ahmed A, Bazaraa A. Three-dimensional analysis of seepage below and around hydraulic structures. ASCE J Hydrol Eng 2009;14(3):243–7.
[33] Alvarez-Aramberri J, Pardo D, Paszynski M, Collier N., On round-off error for adaptive finite element methods. In: Proceedings of the international conference on computational science, ICCS 2012, 2012.
[34] Von Neumann J, Goldstine H. Numerical inverting of matrices of high order. Bull Am Math Soc 1947;53(11):1021–99.
[35] Turing A. Rounding-off errors in matrix processes. Q J Mech Appl Math 1948;1(1):287–308.
[36] Wilkinson J, Laboratory GNP. Rounding errors in algebraic processes. London: Her Majesty's Stationery Office; 1963.
[37] Isaacson E, Keller H. Analysis of numerical methods. New York: Dover Pubns; 1994.